Order parameter coupling and chirality of domain walls

1991 J. Phys.: Condens. Matter 3 5163

(http://iopscience.iop.org/0953-8984/3/27/009)

J. Phys.: Condens. Matter 3 (1991) 5163–5169. Printed in the UK

Order parameter coupling and chirality of domain walls

B Houchmandzadeh†, J Lajzerowicz† and E Salje†‡
† Université Scientifique et Médicale de Grenoble, Laboratoire de Spectrométrie Physique, Boite Postale No 53, F-38041 Grenoble, France
‡ Department of Earth Sciences, University of Cambridge, Cambridge CB2 3EQ, UK

Received 22 January 1991

Abstract. Biquadratic coupling between two order parameters Q_1 and Q_2 can lead to transitions between a phase with only one of the two order parameters active (phase I or II) and a mixed phase III in which both order parameters are symmetry breaking. Domain walls for positive coupling energies are chiral under thermodynamic conditions close to the transition points I–III and II–III. Annihilation of chirality in the wall leads to wall widening and wall bifurcations. The widths of the walls are different for the two order parameters leading to greater lattice distortions on either side of the wall than in the centre of the wall.

1. Introduction

Many phase transitions relate to more than one thermodynamic degree of freedom, each of which leads to symmetry breaking. Typical examples are orientational disorder in $NaNO_3$ with two critical points in the Brillouin zone Z and F (Schmahl and Salje 1989, Harris *et al* 1990), cation ordering and lattice distortions in $CaAl_2Si_2O_8$ (Redfern 1990, Salje 1987) and competition between two improper ferroelastic phase transitions in $Pb_3(PO_4)_3$ and related compounds (Bismayer *et al* 1982, Joffrin *et al* 1979, Salje *et al* 1983) and further examples compiled by Salje (1990). In all these cases, a quantitative description of the temperature evolution of the order parameter in the uniform state was achieved within the general scope of Landau theory using the analysis proposed by Salje and Devarajan (1986). The coupling energies are, for symmetry reasons, biquadratic, i.e. $\lambda Q_1^2 Q_2^2$.

It is in the nature of such non-linear coupling phenomena than even energetically small contributions of a coupled anharmonicity change the phase transition behaviour dramatically. Positive coupling constants, for example, often lead to stepwise transitions (trigger efect) even when the uncoupled processes are continuous. The correlated question, which has so far not been addressed, is how the local order parameters near domain walls react to such coupling phenomena. Here we report that the response of the wall structure is to develop chirality in the order parameter space close to the transition point even if such chirality does not exist in either phase far from the transition point. Effects of chirality in the context of transitions between Ising walls and Bloch walls for equilibrium systems were reported by Bulaevski and Ginzburg (1964) and Lajzerowicz and Niez (1978, 1979); non-equilibrium systems were studied by Coullet *et al* (1990). Here we argue that chiral walls are also a fingerprint for coupling phenomena

0953-8984/91/275163 + 07 $03.50

between order parameters of different symmetry. For discussion of closely related 'non-topological solitons' we refer the reader to the excellent papers of Magyari and Thomas (1984, 1986).

2. The model

Following the nomenclature of Salje and Devarajan (1986), we consider the Gibbs free energy expression

$$G = \tfrac{1}{2}\gamma_1(\nabla Q_1)^2 + \tfrac{1}{2}\gamma_2(\nabla Q_2)^2 + \tfrac{1}{2}A_1Q_1^2 + \tfrac{1}{4}B_1Q_1^4 + \tfrac{1}{2}A_2Q_2^2 + \tfrac{1}{4}B_2Q_2^4 + \lambda Q_1^2Q_2^2.$$

The coupling constant, λ, is positive and we consider the transition between the phase I ($Q_1 \neq 0, Q_2 = 0$) and phase III (both order parameters non-zero); the phase transition occurs at the critical point

$$A_2^{(\text{uniform})} = 2\lambda A_1/B_1.$$

We can now calculate the marginal stability of the domain walls in which two order parameters are active. The pure phase I become unstable with respect to the paraphase $Q_1 = Q_2 = 0$ at $A_2 = 0$. The interval in which both order parameters are locally permitted is, thus limited by $2\lambda A_1/B_1 < A_2 < 0$. The Euler–Lagrangian equation in the friction limit of the wall is

$$\mathrm{d}Q_1/\mathrm{d}t = -A_1Q_1 - B_1Q_1^3 + \gamma_1\nabla^2Q_1 - 2\lambda Q_1Q_2^2$$

$$\mathrm{d}Q_2/\mathrm{d}t = -A_2Q_2 - B_2Q_2^3 + \gamma_2\nabla^2Q_2 - 2\lambda Q_1^2Q_2.$$

In the stability field of phase I, we can solve this equation with

$$Q_1 = (^*A_1/B_1)\,\tfrac{1}{2}\tanh(-A_1/2\gamma_1)^{1/2}x = Q_1^{(0)}$$

$$Q_2 = 0$$

where x is the coordinate perpendicular to the wall. Approaching the critical pint, the wall profile will be modified by a variation εq

$$Q_1 = Q_1^{(0)} + \varepsilon q_1 \qquad Q_2 = \varepsilon q_2.$$

The relevant parameter Q_2 then follows from

$$\mathrm{d}q_2/\mathrm{d}t = (-A_2 + 2\lambda A_1/B_1 \tanh^2 \alpha z)q_2 + \gamma_2\nabla^2 q_2.$$

This equation is formally identical to a Schrödinger equation with the relevant eigenvalue of (Landau and Lifshitz 1980)

$$E = -A_2 + 2\lambda A_1/B_1 + A_1\gamma_2/(8\gamma_1)[1 - (1 + 16\lambda\gamma_1/B_1\gamma_2)^{1/2}].$$

For small values of the coupling constant, we can develop all terms in $\lambda\gamma_1/B_1\gamma_2$ and find for the marginal stability $E = 0$ ($E < 0$ for Ising walls, $E > 0$ for chiral walls) a value for A_2

$$A_2^{(\text{wall})} = A_2^{(\text{uniform})} - (\gamma_2/8\gamma_2)(-1 + \sqrt{1 + 16\lambda\gamma_1}/B_1\gamma_2)^2A_1$$

where $A_2^{(\text{uniform})}$ is again the value at the phase transition I–III in the uniform case.

A typical set of parameters used for the following analytical work is $A_1 = -1$, $\lambda = 0.1$. The model parameter is A_2 which is varied between -2 and 0.2; the uniform phase transition occurs at $A_2 = -0.239$. All other parameters are set to unity.

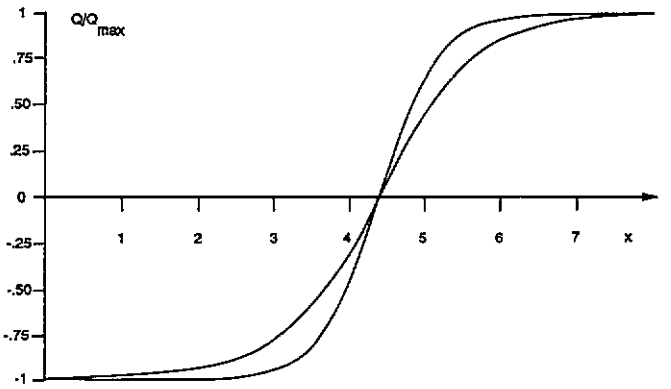

Figure 1. Wall profiles for two coupled order parameters. Both order parameters form kinks, the wall thicknesses are different for the two profiles ($A_2 = -2$).

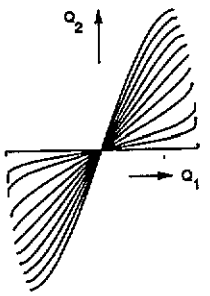

Figure 2. Trajectories of the kink wall profiles for different values of the temperature-related model parameter A_2. (A_2 changes from 0.2 (horizontal line) to -0.4 in steps of 0.1, then from -0.6 to -2 (steepest curve) in steps of 0.2).

3. Wall profiles and trajectories

Three types of walls exist in the phase III with trajectories between the four stable points in the order-parameter space (Q_1, Q_2), $(-Q_1, -Q_2)$, $(-Q_1, Q_2)$ and $(Q_1, -Q_2)$. We first discuss the wall profile between (Q_1, Q_2) and $(-Q_1, -Q_2)$. In figure 1 the wall profiles for both order parameters are shown. As the wall thickness depends on both the uniform term and the gradient energy, it is clear that these two components of the wall have different thicknesses. These differences between the wall thicknesses are clearly born out by the trajectories in figure 2, which show a linear correlation only if the two wall profiles are proportional to each other. A downward bend of the trajectory indicates that the wall in Q_1 is larger than in Q_2 and vice versa for an upward bend. Phase I is characterized by the horizontal line $Q_2 = 0$.

We can now relate this non-linear trajectory to the chirality of the wall. First we define the chirality via the gradient of the angle between the two order parameters in order-parameter space. The gradient is taken in the direction perpendicular to the wall. A measure for this gradient is the Lifshitz term

$$\chi = Q_1 \, \mathrm{d}Q_2/\mathrm{d}x - Q_2 \, \mathrm{d}Q_1/\mathrm{d}x$$

which is zero for non-chiral walls. Kinks with two different wall thicknesses in Q_1 and Q_2 have a non-zero Lifshitz term and are chiral. As the kinks have a common inversion centre in the middle of the wall, the chirality changes sign on one side of the wall

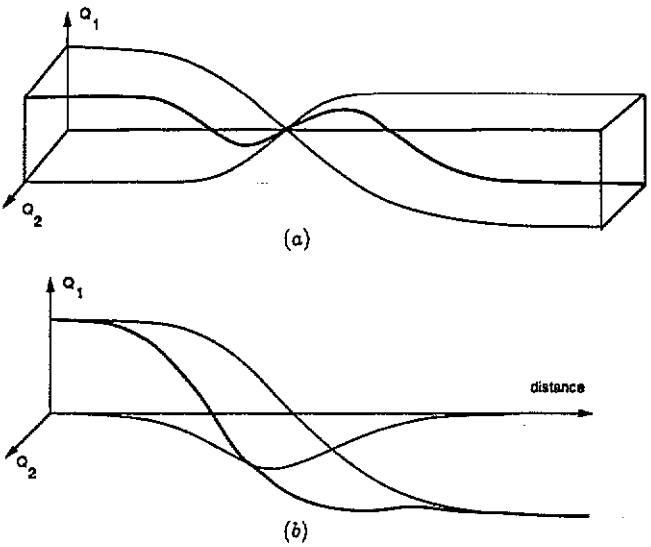

Figure 3. Sketch of bi-chiral and single-chiral walls. The two order parameters Q_1 and Q_2 are plotted as orthogonal vectors on the left-hand side. The bi-chiral wall (*a*) is the vector sum $Q_1 + Q_2$ of two primary kinks in Q_1 and Q_2 with two different wall thicknesses $w_1 \neq w_2$. The single-chiral wall (*b*) is the sum of a kink wall (Q_1) and a breather (Q_2). The resulting wall profiles are shown as thick curves.

compared with its sign on the other. The total chirality is zero and we call these walls 'bi-chiral' (or 'dipolar chirality'). The opposite case is when the sign of chirality does not change in the wall (i.e. 'single chirality'). This case is discussed below. This situation is illustrated by the sketch of the two wall profiles in figure 3(*a*). Here the order parameters are shown in the 'order parameter vector space' together with their spatial evolution with distance from the bulk solution on the left and right end of the drawing. Both profiles follow a tanh behaviour with different effective wall thicknesses. The vector sum of the two order parameters is shown as a thick line representing the true wall profile. This wall is 'bi-chiral'.

The difference between the wall thicknesses of the two components of the wall can be relevant for the understanding of effects like decoration and early stages of exsolution in twinned crystals. The exsolved species will enrich at the position of lowest chemical potential, which is related to the square of the order parameters. Under suitable coupling conditions with the local strain, one can find the maximum lattice distortion to be related to $Q_1^2 - Q_2^2$. In order to visualize the effect, we normalize each order parameter to unity in the uniform state and plot the difference function of the squared order parameters in figure 4. This function is double-peaked with a maximum at either side of the wall and a local minimum in the middle of the wall. Decoration, such as Sr or U in ternary feldspars (e.g. Smith 1974) may now occur on these maxima of the lattice distortion. It is interesting to note that this fine structure of the wall profile depends sensitively on the thermodynamic conditions under which the wall is produced and it might well be that such decoration effects can be used for geological fingerprinting.

We now discuss the case of single chirality for walls between the states (Q_1, Q_2) and $(-Q_1, Q_2)$. The repulsive coupling ($\lambda > 0$) in the model leads to competition between the two order parameters so that one order parameter reduced the other. As one order

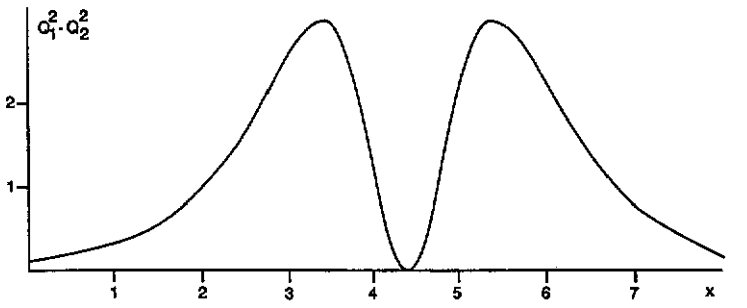

Figure 4. Profile of the function $Q_1^2 - Q_2^2$ for $A_2 = -2$. We may expect that decoration of walls follows this double-peaked profile with enrichment of defects at the two maxima but not in the middle of the wall.

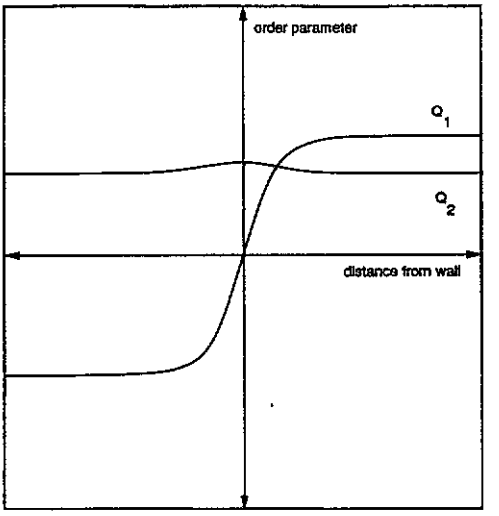

Figure 5. Chiral wall with the two components Q_1 (kink, odd symmetry) and Q_2 (breather, even symmetry) ($A_2 = 0.6$).

parameter vanishes in the wall, the other will increase. The vanishing order parameter must have odd symmetry with respect to the mirror symmetry of the wall, whereas the order parameter bond to the wall must have even symmetry. It is clear that this situation leads to chirality. In figure 5 the wall profiles are shown for the numerical calculations. The order parameter Q_1 follows the kink behaviour (odd symmetry); the order parameter Q_2 shows a breather profile (even symmetry). The width of the kink is smaller than the width of the breather because the gradient energy smoothes the breather more effectively than the kink. When the temperature related parameter A_2 is reduced so that Q_2 disappears in the uniform case, we still find non-zero values of Q_2 in the breather (figure 6). The trajectories are shown in figure 7. In order-parameter space, the wall is now fully chiral because the order parameter Q_2 disappears outside the breather (figure 3(*b*)). The wall is characterized by a rotation of the order parameter from $+Q_1$ in the uniform matrix through Q_2 in the wall to $-Q_1$ in the uniform matrix on the other side of the wall. The sense of the chirality does not change in the wall.

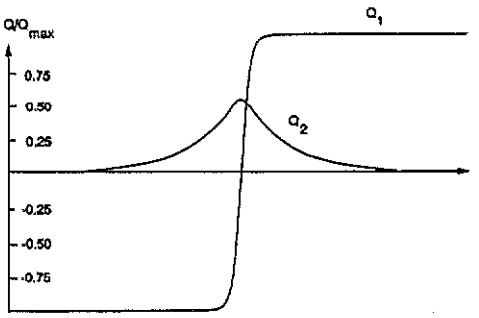

Figure 6. Wall profiles within the marginal stability of phase III ($A_2 = -0.2$). The bulk material on either side is in phase I ($Q_2 = 0$, $Q_1 \neq 0$). The wall is the combination of a kink (Q_1) and a breather (Q_2) and is single chiral.

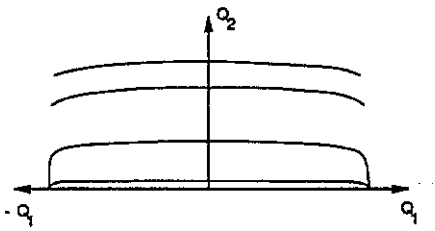

Figure 7. Trajectories of wall profiles of the type shown in figure 5 and 6. The walls are pure kinks (horizontal line) in phase I under conditions far from the transition point. Strong chirality develops in phase I close to the transition point (half moon, touching the horizontal line). Weak chirality appears in phase III with slightly bent trajectories shifted to positive values of Q_2.

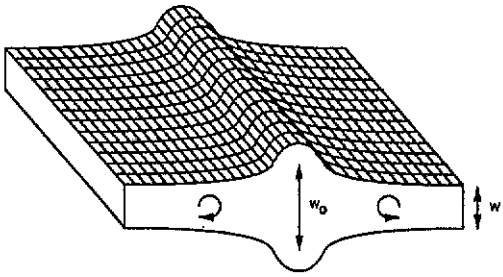

Figure 8. Wall profile close to a line of compensated chirality.

A similar behaviour was found by Coullet *et al* (1990) for the transition between an Ising wall and a Bloch wall. Quantitative differences arrive in our model because we find in general that the wall thicknesses of the two components are different so that Q_2 increases well outside the wall thickness of Q_1.

Stressing the generality of our findings leaves us with the difficulty of their direct experimental observation. Inspection of images of ferroelastic materials with two competing order parameters as obtained from transmission electron microscopy seem to show singularities in walls which could relate to chirality. The optimal image conditions are, however, difficult to maintain and the observation may be hampered by the influence of defects and wall interactions.

4. Annihilation of chirality and wall bifurcations

Let us now consider a kink in Q_1 which has single chirality. There are two possibilities for the sense of the chirality depending on the sign of Q_2 in the wall. The two solutions are degenerate because the Euler–Lagrangian equation for $Q_2^{(0)} = 0$ is invariant with respect to the sign of q_2. We can now envisage two parts of the same wall with respect to Q_1 but opposite chirality (e.g. 'right' for $Q_2 > 0$ and 'left' for $Q_2 < 0$). The two

chiralities cancel at the junction where the two parts of the wall meet. This junction forms a line in the wall with $Q_2 = 0$ and $Q_1 = 0$. The structural elements on this line are those of the paraphase, where both order parameters vanish. Moving away from the line, the symmetry of both Q_1 and Q_2 is odd so that wall junctions and wall crossings are symmetry allowed on the line.

The width, w_1, of the wall in Q_1 is determined by the gradient energy and the linear term in the Euler–Lagrangian equation of Q_1

$$w_1 = [\gamma_1/(-A_1 - 2\lambda Q_2^2)]^{1/2}$$

and depends explicitly on the value of Q_2 in the wall. A wall forms only for positive values of the denominator, i.e. for negative values of A_1. With $\lambda > 0$, the role of Q_2 is to reduce the wall thickness. This reduction of the wall thickness is cancelled at the line of vanishing chirality where $Q_2 = 0$. As a consequence, the wall width increases locally and the wall bulges out to both sides (figure 8). The diameter of the bulge is $(\gamma_1/-A_1)^{1/2}$, which is the same as would occur without order-parameter coupling. In situations where the stability field of the phase I is small (i.e. $A_1 \simeq 0$), the wall thickness diverges locally. A second wall is then established perpendicular to the first. This second wall is again chiral and the same local compensation of chirality and wall divergence occurs in this wall. We expect in this case a network of wall to form that is not unlike that of tweed textures of orthogonal walls.

In conclusion, we wish to point out that the role of the anihilation line (i.e. the line of vanishing chirality) in increasing the local wall thickness can be understood as a prewetting phenomenon. It increases the dimension of the line $d = 1$ to $d = 2$ on the wall in the same way as the uniform increase of the wall thickness ($d = 2$) is the precursor of the phase transition that takes place in the 3D bulk.

Acknowledgments

ES thanks the University of Grenoble for its hospitality during his visit 1990/91 and the Leverhulme trust for support.

References

Bismayer U, Salje E and Joffrin C 1982 *J. Physique* **43** 1378
Bulaevski L N and Ginzburg V L 1964 *Sov. Phys.-JETP* **18** 530
Coullet P, Lega J, Houchmandzadeh B and Lajzerowicz J 1990 *Phys. Rev. Lett.* **65** 1352–5
Harris M J, Salje E and Güttler B 1990 *J. Phys.: Condens. Matter* **2** 5517
Joffrin C, Benoit J P, Currat R and Lambert M 1979 *J. Physique* **40** 1185
Lajzerowicz J and Niez J J 1978 *Solitons and Condensed Matter Physics* ed A R Bishop and T Schneider (Berlin: Springer)
—— 1979 *J. Physique Lett.* **40** L165
Landau L D and Lifshitz E M 1980 *Quantum Mechanics* (Oxford: Pergamon)
Magyari E and Thomas H 1984 *Phys. Lett.* **100A** 11
—— 1986 *Helv. Phys. Acta* **59** 845
Redfern S A T 1990 *Phase Transitions in Ferroelastic and Co-elastic Crystals* (Cambridge: Cambridge University Press)
Salje E 1987 *Phys. Chem. Minerals* **14** 181
—— 1990 *Phase Transitions in Ferroelastic and Co-elastic Crystals* (Cambridge: Cambridge University Press)
Salje E and Devarajan V 1986 *Phase Transitions* **6** 235
Salje E, Devarajan V, Bismayer U and Guimaraes D M C 1983 *J. Phys. C: Solid State Phys.* **16** 5233
Schmahl W W and Salje E 1989 *Phys. Chem. Minerals* **16** 790
Smith J V 1974 *Feldspar Minerals* (Heidelberg: Springer)